

Indoor MIMO Transmissions with Alamouti Space-Time Block Codes

Sebastian Caban, Christian Mehlführer, Arpad L. Scholtz, and Markus Rupp

Vienna University of Technology
Institute of Communications and Radio-Frequency Engineering
Gusshausstrasse 25/389, A-1040 Vienna, Austria
http://www.nt.tuwien.ac.at/rapid_prototyping
{scaban, chmehl, ascholtz, mrupp}@nt.tuwien.ac.at

ABSTRACT

Research on Alamouti's space-time coding algorithm up to now was primarily based on numerical simulations *simplifying* the transmission channel in a skillful manner. To close the gap between simulation and reality, ever more sophisticated channel models are developed. This leads to increased simulation time and algorithmic complexity. But it remains an open question whether reality is reflected sufficiently well.

As a contribution to the answer of this question, we present the hardware implementation of a 2.45 GHz MIMO transmission system utilizing Alamouti space-time coding. We carry out MIMO measurements in several typical indoor scenarios. In terms of BER over SNR performance, we compare the measurement results obtained with numerical simulations. Good agreement with previously published simulation results is observed.

1. MOTIVATION

Transmit and receive diversity have emerged as effective means of achieving higher throughput in wireless communication systems. Space-time block codes try to exploit the presence of independent multipath propagation to improve the reliability of transmission [1]. One popular representative of these codes is the Alamouti scheme [2]. It is well investigated by computer simulations utilizing channel models.

Real scenarios, however, are not as straightforward as models. There are many real-world properties that have an impact on the performance of MIMO transmission. In addition to the radio channel itself, antenna properties like mutual

coupling [3] and uncertainties in MIMO decoding algorithms also influence the performance of transmission [4]. These uncertainties are due to assumptions like uncorrelated additive Gaussian noise, ideal power amplification, exact synchronization, known noise levels, and perfect channel knowledge.

In other words, state-of-the-art MIMO channel models greatly simplify the reality but try to cover all of its important aspects. Relying on simulation as the *only* tool for performance investigation of MIMO transmission, however, leaves questions unanswered:

- Are there any important aspects of the transmission chain that have been overlooked?
- How closely does the channel model reflect the reality?
- How simple can we keep the channel model to still reflect the reality sufficiently well?
- What impact does the radio frequency frontend have on the measurement results?

To seek answers, we have implemented a complete MIMO transmission system utilizing Alamouti [2, 5] space-time coding.

The experimental setup is described in the next section. Measurement results are presented and compared to simulations in Section 3. Finally, conclusions are drawn in Section 4.

2. EXPERIMENTAL SETUP

The measurements were carried out using our existing MIMO testbed [6]. Baseband signal processing was implemented in MATLAB on a user PC that interfaces the transmit and receive PC via a local area network connection (see Figure 1). The signal implementation for BER over SNR measurement is described in the following.

This work has been funded by the Christian Doppler Laboratory for Design Methodology of Signal Processing Algorithms. (<http://www.nt.tuwien.ac.at/cdlab/>)

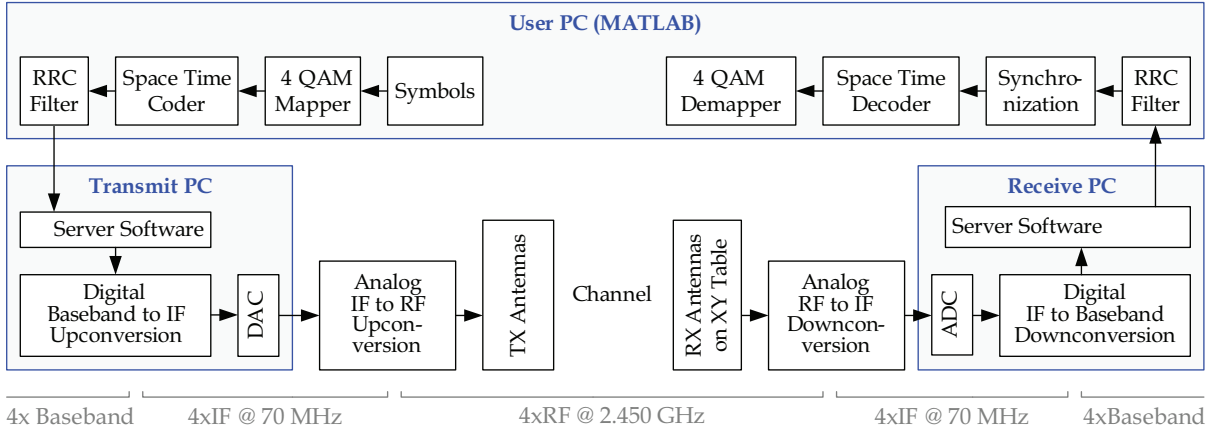


Fig. 1: Measurement setup.

2.1. Transmitter

At first, 700 quaternary, equally probable random numbers (the data to be transmitted) are created in MATLAB and mapped onto a 4 QAM constellation such that the possible symbol values are $1 + j$, $1 - j$, $-1 + j$, and $-1 - j$. Alamouti space-time coding is performed by taking two consecutive symbols $\{s_1, s_2\}$, and sending the sequence $\{s_1, s_2^*\}$ on the first and $\{s_2, -s_1^*\}$ on the second antenna¹. To allow for phase and timing recovery at the receiver, a training sequence is added as a header to the data. Orthogonal gold sequences are used for each transmit antenna. The training and data sequence next are root raised cosine (RRC) filtered (rolloff=0.22) before they are transferred to the transmit hardware.

The data samples are interpolated and digitally upconverted to an intermediate frequency (IF) of 70 MHz in real-time. IF filters, analog upconversion to 2.45 GHz, and amplification to a maximum transmit power of -10 dBm (signal bandwidth = 1.9 MHz) are followed by two $\lambda/4$ -monopole ground-plane antennas spaced approximately 0.5λ ².

2.2. Channel

We studied typical non line of sight (NLOS) and line of sight (LOS) scenarios in a corridor and its adjacent rooms. Because we experienced interference with omnipresent wireless LAN networks operating in the same frequency, we decided to place the setup into the basement where this interference did not exist anymore.

While the transmit antenna array (e.g. representing a wireless hotspot) is fixed to a specific location, the receive antenna array (e.g. represent-

ing user equipment) is moved using an xy positioning table. For the averaging process over a small scale fading scenario, we measured in increments of 0.11λ along a $2.5\lambda \times 2.5\lambda$ sized grid. This resulted in 506 channel realizations.

2.3. Receiver

As at the transmitter, 0.5λ spaced $\lambda/4$ -monopole ground-plane antennas are also used at the receiver. Up to four receive antennas are available.

The received signals are pre-filtered, analog downconverted to an intermediate frequency of 70 MHz, and then amplified to match the signal levels needed by the analog to digital converter stage. After decimation and digital downconversion, the baseband data samples are filtered by a matched root raised cosine filter and then transferred back to the user PC performing the receiver algorithms in MATLAB.

First, the complex baseband data samples are correlated with the training sequence to synchronize them in time and phase. Next, the channel matrix \mathbf{H} (size: $N_r \times N_t$) is estimated by using a least squares estimator [7]

$$\hat{\mathbf{H}} = \mathbf{T}_r \mathbf{T}_t^H (\mathbf{T}_t \mathbf{T}_t^H)^{-1}, \quad (1)$$

where \mathbf{T}_t (size: $N_t \times N_{\mathbf{T}}$) denotes the transmitted and \mathbf{T}_r (size: $N_r \times N_{\mathbf{T}}$) the received $N_{\mathbf{T}}$ training symbols for all N_t transmit and N_r receive antennas. Once $\hat{\mathbf{H}}$ is known, the SNR at the receiver is estimated and space-time decoding is performed. To this end, we introduce a virtual channel matrix

$$\hat{\mathbf{H}}_v = \begin{bmatrix} \hat{\mathbf{h}}_1 & \hat{\mathbf{h}}_2 \\ -\hat{\mathbf{h}}_2^* & \hat{\mathbf{h}}_1^* \end{bmatrix} \quad (2)$$

where $\hat{\mathbf{h}}_1$ denotes the first column of the estimated channel matrix $\hat{\mathbf{H}}$ and $\hat{\mathbf{h}}_2$ the second. The receive vector \mathbf{r} is formed by stacking consecutive data samples $\mathbf{r}_1, \mathbf{r}_2, \dots$ of all N_r receive antennas (e.g.

¹ We use * to denote conjugation, T to denote matrix transposition, and H to denote conjugate matrix transposition. \hat{X} denotes the estimated value of X .

² The wavelength λ for 2.45 GHz is approximately 12.2 cm.

$\mathbf{r}_1 = [r_{11}, r_{12}, \dots, r_{1N_r}]^T$) in the following way:

$$\mathbf{r} = \begin{bmatrix} \mathbf{r}_1 \\ \mathbf{r}_2^* \end{bmatrix} \quad (3)$$

For the Alamouti code it can be shown that the maximum likelihood receiver minimizing the metric

$$\|\mathbf{r} - \hat{\mathbf{H}}_v \mathbf{s}\|^2 \quad (4)$$

over all possible transmit vectors \mathbf{s} performs equally to the zero forcing receiver

$$\hat{\mathbf{s}} = (\hat{\mathbf{H}}_v^H \hat{\mathbf{H}}_v)^{-1} \hat{\mathbf{H}}_v^H \mathbf{r} \quad (5)$$

which was used to estimate the transmitted symbols $\hat{\mathbf{s}}$. Finally, the BER is evaluated by comparing the transmitted bits with the received bits.

2.4. Obtaining BER over SNR Curves

The transmission of a *single* data block in a specific scenario yields two results: an estimated SNR and a BER. This measurement is repeated for all channel realizations which are created by moving the receive antenna using the xy positioning table. The resulting SNRs and BERs are averaged to represent a single measurement point in a BER over SNR curve.

Different average SNR values are created by changing the transmit power in steps of 2 dB and repeating the procedure described above.

Some 20 minutes are needed to transmit and receive data for a complete BER over SNR figure with five curves (five different codes) and 20 different average SNR values. The evaluation of the resulting 20 GB of baseband data takes about two additional hours.

3. MEASUREMENTS

In the following, we present our measurement results. More than 30 different scenarios were investigated in several measurement campaigns.

3.1. 2×1 Alamouti with Rayleigh fading

In a specific indoor NLOS scenario with Rayleigh fading, we measured the BER over SNR performance of a SISO link in comparison to 2×1³ Alamouti coded transmission. Each circle in Figure 2 represents the BER and SNR averaged over 506 measurements.

The thin, solid lines represent the theoretical results [8] for a Rayleigh fading channel with i.i.d.⁴ channel coefficients and additive Gaussian noise.

The dashed lines represent a baseband simulation using the channel matrices $\hat{\mathbf{H}}$ and the noise

³ 2×1: two transmit antennas and one receive antenna

⁴ i.i.d. = independent identically distributed

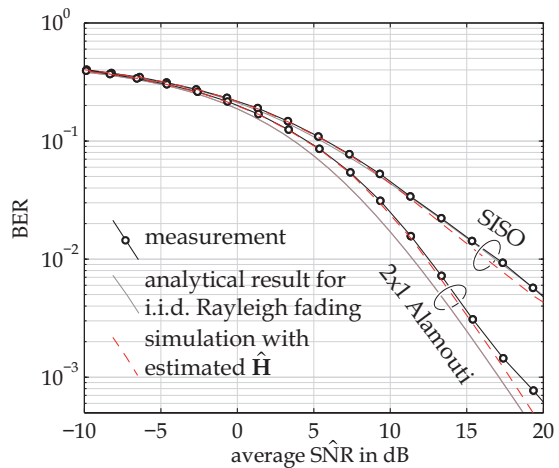


Fig. 2: Indoor NLOS scenario with Rayleigh fading.

variance estimated in the corresponding measurement. Assuming perfect channel knowledge and additive Gaussian noise, the received data is calculated as $\mathbf{S}_r = \hat{\mathbf{H}}\mathbf{S}_t + \mathbf{N}$. Baseband simulation such obtained closely matches the measurement results. This finding shows that the BER over SNR performance of an Alamouti code can be calculated by baseband simulation using the “right” channel matrices and additive Gaussian noise.

The measured performance in Figure 2 differs from the analytical result for an i.i.d. Rayleigh channel for the following reasons:

- The channel coefficients turned out to be independently Rayleigh distributed but with a 6 dB different⁵ variance σ^2 . This moves the BER curve towards the SISO case.
- Taking the average over just 506 channel realizations leads to some tolerance in the results⁶. No systematic deviation was observed.

3.2. 2×1 Alamouti with Ricean fading

In our measurement campaign, typical indoor scenarios often showed a behavior better characterized by Ricean fading than Rayleigh fading. A measurement obtained in such a scenario is depicted in Figure 3.

Again, the simulated results using the channel matrices from the measurements (dashed lines) very closely match the measured performance. Due to the Ricean fading, the link performance is substantially better than in the Rayleigh fading case.

⁵ The transmit power for both antennas was nearly equal, but in this particular measurement scenario, the fading was such that one antenna performed pronouncedly better.

⁶ The curves in the figures are so smooth because the measurements for all different SNRs are obtained from the same channel realizations.

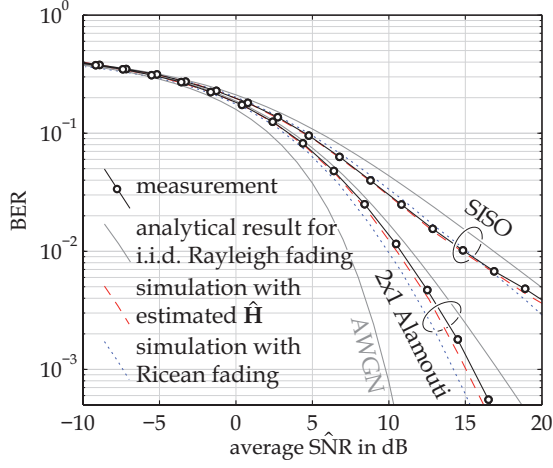


Fig. 3: Indoor NLOS scenario with Ricean fading ($K=[1.4, 2.5]$).

The dotted curve in Figure 3 was obtained by a simulation assuming independent Ricean fading of the channel coefficients and additive Gaussian noise. The variance σ^2 and the K-factor⁷ of the Ricean distribution were estimated independently for each of the two transmit antennas by maximum likelihood estimation:

$$\sigma^2 = [10.9 \quad , \quad 14.4] \quad K = [1.4 \quad , \quad 2.5]$$

The NLOS fit in Figure 4 shows the corresponding Weibull probability plot for the distribution of the channel coefficients for the first transmit antenna ($K=1.4$).

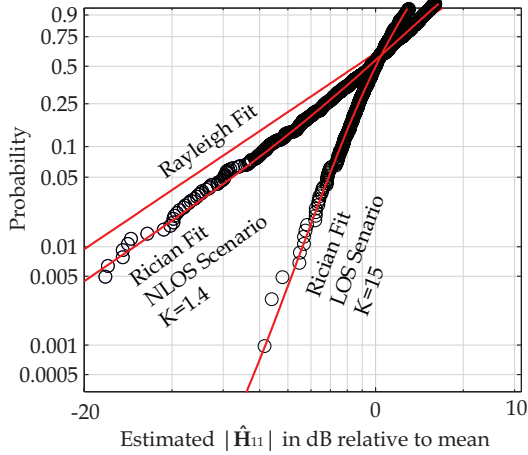


Fig. 4: Weibull probability plot for two different typical indoor scenarios.

Most indoor NLOS scenarios showed a small specular component (usually K was smaller than 1.5).

⁷ Ricean K-factor: ratio of specular to diffuse fading signal power, $K = \frac{s^2}{\sigma^2}$ given pdf(x) = $\frac{x}{\sigma^2} e^{-\frac{x^2+s^2}{2\sigma^2}} I_0\left(\frac{xs}{2\sigma^2}\right)$

This can be explained by the presence of a main signal path.

3.3. 2×1 Alamouti in scenarios with high K-factor

Some NLOS scenarios, where transmitter and receiver were placed in adjacent rooms, showed Ricean fading with high K-factors. In Figure 5, a Ricean K-factor of 5.0 for the link from the first transmit antenna and 2.1 from the second was estimated. The 2×1 Alamouti link still performs better than the SISO link.

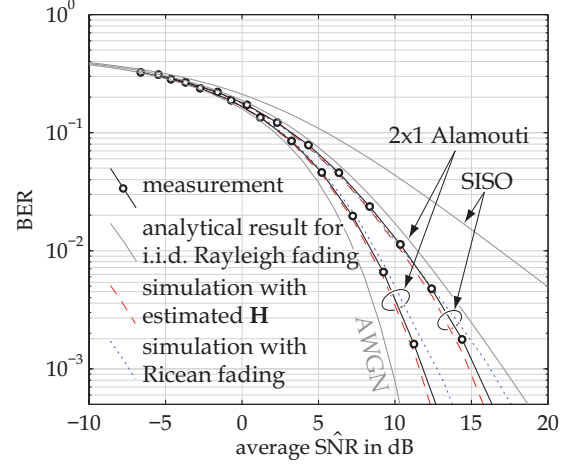


Fig. 5: Indoor NLOS scenario with Ricean fading ($K=[5.0, 2.1]$).

Finally, we set up transmitter and receiver in the same corridor in an LOS scenario ($K=[15, 15]$). Now the SISO link performed as good as the Alamouti link. And again, the results agree with baseband simulation assuming independent Ricean fading and additive Gaussian noise (see Figure 6).

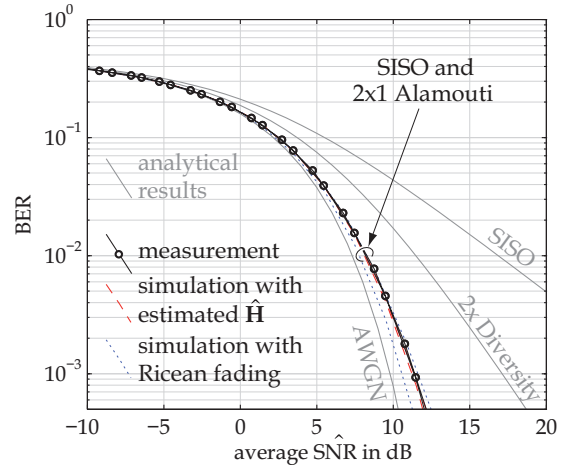


Fig. 6: Indoor LOS scenario Ricean $K=[15, 15]$

3.4. Alamouti with more than one receive antenna

We compared the performance of 2×2 Alamouti coding with a standard 1×2 link, both utilizing maximum ratio combining at the receiver. Figure 7 shows such a comparison for a Rayleigh fading scenario. The measurement results closely fit the theoretical results for independently distributed Rayleigh channels with additive i.i.d. Gaussian noise.

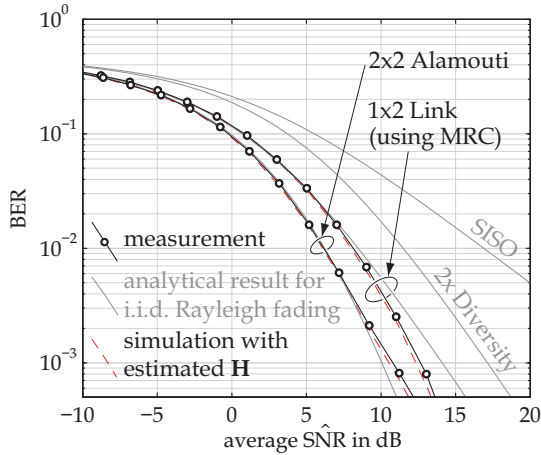


Fig. 7: Indoor NLOS measurement in a scenario with Rayleigh fading.

In Figure 8, the BER over SNR performance of SISO transmission versus Alamouti transmission utilizing 1 to 4 receive antennas can be seen. In this particular scenario, Ricean fading with K factors smaller 0.5 was observed.

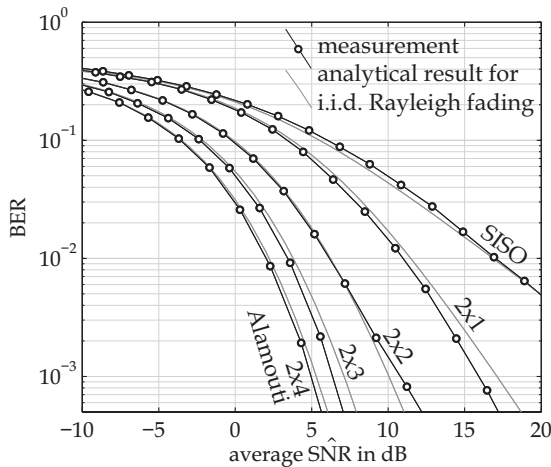


Fig. 8: Indoor NLOS measurement in a scenario with Rayleigh fading.

As already mentioned, in some indoor scenarios, a dominant signal path from the transmitter to the receiver occurred. Figure 9 shows the mea-

surement result for an 2×4 NLOS scenario with the estimated Ricean K-factors of:

$$\hat{\mathbf{K}} = \begin{bmatrix} 5.0 & 1.1 \\ 8.1 & 1.4 \\ 3.6 & 0.4 \\ 2.2 & 0.8 \end{bmatrix}$$

where $[\hat{\mathbf{K}}]_{ik}$ denotes the link between the k^{th} transmit and the i^{th} receive antenna. Such a result with high K-factors was not unusual if the transmitter and receiver were placed in adjacent rooms.

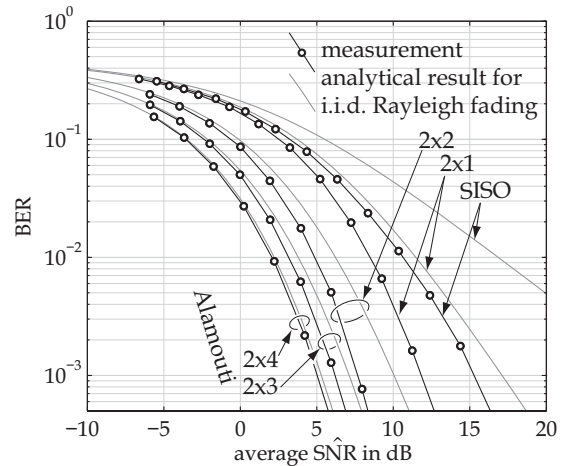


Fig. 9: Indoor NLOS measurement in a scenario with Ricean fading.

Simulation utilizing Ricean fading, with the statistical parameters estimated from the measurements, matches these results (see Figure 10).

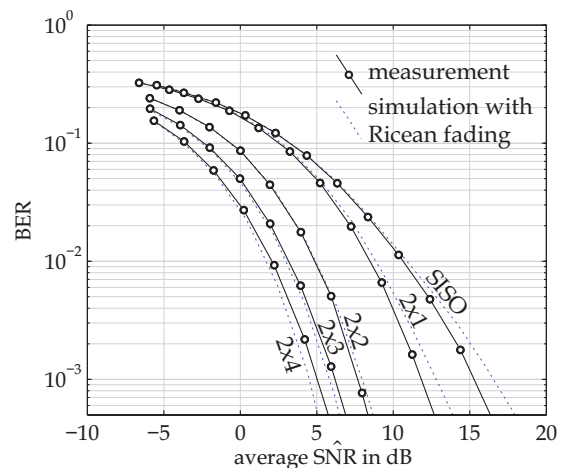


Fig. 10: Indoor NLOS measurement in a scenario with Ricean fading.

4. CONCLUSION

We have implemented a MIMO transmission system in hardware, utilizing Alamouti space-time coding. Using monopole antennas with a spacing as small as $\lambda/2$, we showed that even under these conditions the correlation between the antennas is negligible, and a MIMO link can achieve a significant performance improvement in comparison to the SISO case. The measured performance of all investigated scenarios reflected the simulations assuming independently distributed Ricean fading and i.i.d. Gaussian noise with good accuracy.

5. ACKNOWLEDGMENT

The authors would like to thank Lukas Mayer, Werner Keim, and Robert Langwieser for their help and suggestions on carrying out the measurements.

6. REFERENCES

- [1] D. Gesbert, M. Shafi, S. Da-shan, P. Smith, and A. Naguib, "From theory to practice: an overview of MIMO space-time coded wireless systems," *IEEE Journal on Selected Areas in Communications*, vol. 22, issue 3, pp. 1716–1719, 2003.
- [2] S. Alamouti, "A simple transmit diversity technique for wireless communications," *IEEE Journal on Selected Areas in Communications*, vol. 16, issue 8, pp. 1451–1458, Oct. 1998.
- [3] G.J.Foschini and M.J.Gans, "On limits of wireless communications in a fading environment when using multiple antennas," *Wireless Personal Communications*, vol. 6, no. 3, pp. 311–335, March 1998.
- [4] M. Rupp, "On the influence of uncertainties in MIMO decoding algorithms," in *Proc. 36th Asilomar Conference on Signals, Systems & Computers*, vol. 1, pp. 570–574, 2002.
- [5] V. Tarokh, H. Jafarkhani, and A. Calderbank, "Space-time block codes from orthogonal designs," *IEEE Transactions on Information Theory*, vol. 45, issue 5, pp. 1456–1467, July 1999.
- [6] S. Caban, C. Mehlführer, R. Langwieser, A. L. Scholtz, and M. Rupp, "MATLAB Interfaced MIMO Testbed," *JASP journal on applied signal processing*, in press.
- [7] J. G. Proakis and M. Salehi, *Communication Systems Engineering*, 1994.
- [8] M. Simon and M. Alouini, "A unified approach to the performance analysis of digital communication over generalized fading channels," in *Proc. of the IEEE*, vol. 86, issue 9, pp. 1860–1877, Sept. 1998.